sciendo

POLISH MARITIME RESEARCH 1 (121) 2024 Vol. 31; pp. 85-93
10.2478/pomr-2024-0009

INVESTIGATING FUEL INJECTION STRATEGIES TO ENHANCE SHIP ENERGY EFFICIENCY IN WAVE CONDITIONS

Hossein Ghaemi [1] *
Hamid Zeraatgar [2]
Mojtaba Barjasteh [2]
[1] Gdansk University of Technology, Institute of Naval Architecure, Poland
[2] Amirkabir University of Technology, Faculty of Maritime Technology, Iran

* Corresponding author: *ghaemi@pg.edu.pl (H. Ghaemi)*

ABSTRACT

The prediction of fuel consumption and resulting transportation costs is a crucial stage in ship design, particularly for conditions involving motion in waves. This study investigates the real-time fuel consumption of a container ship when sailing in waves. The overall ship performance is evaluated using a novel non-linear coupled hull-engine-propeller interaction model. A series of towing tank experiments for hull resistance in waves and propeller performance are conducted. The ship engine is mathematically modelled by a quasi-steady-state model equipped with a linear Proportional-Integrator (PI) governor. Various scenarios of shipping transportation are studied, and the resulting instantaneous fuel consumptions and their correlation to other dynamic particulars are demonstrated. Additionally, daily fuel consumption and fuel cost per voyage distance are presented. It is also shown that the controller can effectively adjust the fuel rate, resulting in minimum fuel consumption. The study concludes that there is no correlation between fuel consumption and the frequency of fuel rates. The present framework and mathematical model can also be employed for ship design and existing ships to predict the total required energy per voyage.

Keywords: Fuel consumption, Energy efficiency, Hull-Engine-Propeller interaction, Ship engine dynamics, Added resistance, Sea wave

INTRODUCTION

More than 80 per cent of all goods transferred are carried over the seas [1]. This results in the consumption of millions of tonnes of fuel every year, costing several million dollars. Higher levels of fuel consumption lead to more gas emissions. Additionally, the expense of shipping is generally governed by the fuel cost for large ships [2]. Therefore, accurate estimates of ship fuel consumption are required. Researchers widely investigate the prediction and reduction of ship fuel consumption. Generally, various methods can be categorized into three distinctive models consisting of white-box models (WBMs), black-box models (BBMs), and grey-box models (GBMs) [3]. In WBMs, or deterministic models, all parameters or determinants are known in advance. The most important parameters are hull resistance, characteristics of the propulsion system, weather conditions, and engine performance [4]. In contrast, BBMs, or machine learning models, are based on the onboard measurement of data during voyages. The system trains on data and becomes more precise with increased data input [5]. The primary apparatus of these models (WBMs and BBMs) is an artificial neural network [6]. The GBMs use some known parameters and start training with data recorded onboard, but are usually established on a statistical approach [7].

The fuel consumption of any vessel is dependent on all its operational parameters, such as ship speed, hull resistance,

draft, trim, loading condition, weather, and sea condition [8]. Once an accurate estimation of fuel consumption is acquired, different methods to reduce this consumption can be investigated. Shipping companies concentrate on two separate methods of reducing fuel consumption, either the design of new ships or retrofitting and operational techniques for existing ships. [9]. The former method, which requires more investment, investigates hulls with lower drag, lighter materials, hybrid engines with improved performance, etc. This method certainly has a stronger contribution to the reduction of fuel consumption compared to operational techniques for existing ships. However, this comes at a higher expense [10]. The latter method is available for all ships which are already built and come at a lower price. This method of reducing fuel consumption does not introduce any major modifications in the main ship systems and mostly emphasizes the optimal use of fuel onboard and voluntary and involuntary speed loss. These techniques include but are not limited to, slow steaming [11], weather routing [12], optimized speed [13], trim optimization [14], and voyage optimization [4]. Using these techniques usually increases the shipping time but reduces fuel consumption. The ship owner should always make a balance between shipping time and consumed fuel in total shipping expenditures. Moreover, there are other criteria, for example, general strength, that should be combined with energy efficiency to select the final solution [15].

Engine dynamics also have a significant impact on fuel consumption. Larsen et al. [16] investigated different configurations of two-stroke, diesel-based machinery systems for large ships. They used uncoupled analytical models of the ship's subsystems, such as engine dynamics, propulsion system, and hull resistance. Yin et al. [17] designed an accurate real-time fuel consumption monitoring system based on the engine speed, its power, and the ship speed. A correlation between generated power and consumed fuel was established. A similar interesting study was also carried out by Sandvik et al. [18], with the results of their simulation found to be in reasonable agreement with onboard full-scale measurement of a cargo ship. Different determinants involving engine dynamics, fuel consumption, speed, position, and wind speed are measured on this ship. Degiuli et al. [19] showed that fuel consumption is increased for a container ship as a function of different speeds and wave frequencies. Engine or propeller dynamics were not included in this study. Tilling and Ringsberg [20] employed a 4-DOF (surge, drift, yaw and heel) model for the prediction of fuel consumption, which considers added resistance. The proposed model incorporates important determinants, but not as a coupled system. It is worth mentioning that the fuel pre-injection and injection processes and systems also have a significant influence on fuel consumption, particularly in unsteady states [21-23].

Most of the mentioned studies cannot simulate the ship dynamics and sea conditions as an integrated system. Thus, the suggested models cannot be easily studied if one of the determinants is changed or generalized for use in other ships. Therefore, their applications are restricted and are also difficult to develop further. To remove this weakness, the present research focuses on establishing a white-box, or deterministic, model, for the prediction of fuel consumption in displacement ships, with a further goal of reducing this fuel consumption to meet the UN's sustainability goals (items 7, 12, and 13) [1]. The ship dynamics and sea conditions are simulated through a non-linear coupled hull-engine-propeller interaction model and all influencing parameters are investigated simultaneously. Ship motion in waves is of more importance due to higher resistance and therefore higher fuel consumption, rather than motion in calm waters.

FORMULATION

The main determinants in this study are hull geometry, engine dynamics, propeller performance, and sea conditions. Although it is complicated to capture this coupled problem in an exact manner, it can be presented with some assumptions [24] using the following 1-DOF (surge) system of equations:

$$\begin{cases} T_n(t) - R_C(u(t)) - R_A(u(t)) = (\Delta + x_{\dot{u}})\dot{u}(t) \\ Q_E(t) - Q_P(t) = (I_P + I_{Pa} + I_E + I_S)\dot{\omega}(t) \end{cases} \quad (1)$$

where R_C, R_A, T_n, Δ, and $x_{\dot{u}}$ are the total ship resistance in calm water, as a function of surge speed, $u(t)$; mean added resistance; net generated thrust; ship mass; and the ship added mass, respectively. The second equation is the engine-propeller interaction stated as the law of angular motion where $Q_E(t)$, $Q_P(t)$, I_P, I_{Pa}, I_E, I_S, and ω are the delivered engine torque; required propeller torque; propeller moment of inertia; propeller added moment of inertia; engine moment of inertia; shaft moment of inertia; and shaft angular speed, respectively. The proposed system of equations introduces five sets of determinants:

1. Ship resistance (both in calm water and sea waves);
2. Propeller characteristics (thrust and torque);
3. Engine dynamics (torque, angular velocity, and controller);
4. Vessel specifications (moments of inertia, mass, and added mass);
5. Ship dynamics (surge speed).

All of these determinants are time-dependent variables, excluding vessel specifications. Thus, the solution of this system of equations results in instantaneous ship response.

SHIP RESISTANCE

When ships sail in waves, the total resistance increases by up to 15–30% compared with calm water sailing [25]. The added resistance considerably influences the ship's motion and its attainable speed, resulting in an increased power requirement and higher fuel consumption. The proposed governing system of equations are capable of estimating additional fuel consumption due to added resistance. The ship resistance in calm waters can be computed using different formulas, such as those recommended by International Towing Tank Conference (ITTC). However,

the calculation of the added resistance is not straightforward because of its dependency on several influencing parameters, such as ship speed, hydrostatic trim, wave frequency, heading angle, wave period, draft, radii of gyration, etc.

To obtain an accurate estimation of added resistance, a series of model test experiments are conducted in a towing tank for a Series 60 with $C_B = 0.6$. The added resistance of the model is computed with a known value of calm water resistance using the following equation:

$$R_{Am}(t) = R_{Tm}(t) - R_{Cm}(t) \tag{2}$$

and usually presented as time-averaged added resistance, $\hat{R}_{Am}$, or mean added resistance:

$$\hat{R}_{Am} = \frac{1}{\Delta T}\int_{t_1}^{t_2} R_{Am}\, dt \tag{3}$$

Here, the subscripts A, m, T, and C stand for the added resistance; model; the total resistance; and calm water resistance, respectively. The full-scale ship added resistance is related to the measured value for model by applying Froude's law of similitude:

$$R_{As}(t) = \lambda^3 \times R_{Am}(t) \tag{4}$$

Hence, R_{As} and λ are the ship added resistance and model length scale, respectively. Table 1 indicates the setup of the model tests.

Tab. 1. Configuration of the model test experiments

Model specification			
Hull offset	C_B	LOA	λ
Series 60	0.6	4.57 m	1:40
Wave dynamics			
Heading	Height	Period	Length
180 deg	8 cm	1.6 sec	4.0 m

The dominant parameter in added resistance studies is the characteristic wavelength, which is defined as the ratio of the wavelength to the ship length. In practice, this is about 0.8–1.1 for long waves [26]. This non-dimensional length is set to $\lambda/L = 4/4.57 = 0.88$ for the present experiments. Resistance, heave and pitch motions, and wave profile are recorded in each run. The measured data is scaled using the law of similarity for a real full-scale ship with the main particulars presented in Table 2.

Tab. 2. Main particulars of the full-scale ship

LOA	Beam	Draft	C_B	Speed	∇
182.9 [m]	24.4 [m]	9.8 [m]	0.6	23.8 [Kn]	26245.4 [m³]

Fig. 1 depicts the calm water resistance and time history of the added resistance for the fullscale ship, scaled from the measured data with a length scale of 1:40.

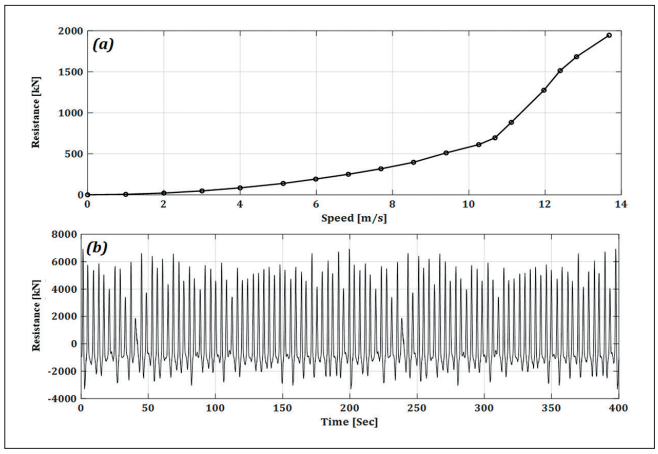

Fig. 1. Full-scale ship resistance, (a) variation of calm water resistance at different surge speeds, (b) time history of the added resistance

PROPELLER CHARACTERISTICS

Additional important determinants are the propeller dynamics, including shaft angular velocity; propeller thrust; and propeller torque. A series of experiments has been conducted for the measurement of the open water performance of the selected propeller. The selected propeller is a fully submerged 5-blade B-Wageningen with a diameter of 25 cm. The experimental setup and measured characteristics are shown in Fig. 2.

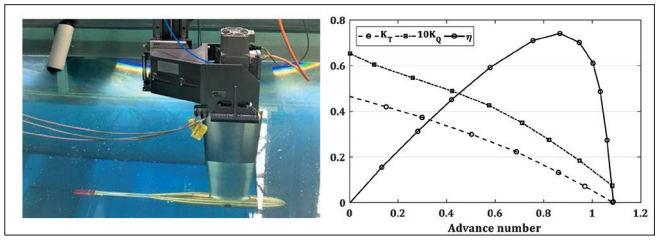

Fig. 2. Propeller open water performance, experimental setup and measured data

The thrust coefficient, K_T, torque coefficient, K_Q, and open water performance, η_0, are measured for different advance numbers, J_P. Table 3 introduces the geometrical specification of the full scaled propeller based on the selected length scale of 1:40.

Tab. 3. Specification of full-scale propeller

Geometry	Type	Diamete	Blades	Area ration	Pitch ration
B-Wageningen	FPP	7.6 m	5	0.58	1.00

To compute the generated thrust of the full-scale propeller, the required torque, and corresponding efficiency, one can use the following set of equations:

$$T_n = (1 - t)\, K_T \rho \omega_p^2 D_P^4 \tag{5}$$

$$Q_P = K_Q \rho \omega_p^2 D_P^5 \tag{6}$$

calculated at different advance numbers, J_P,

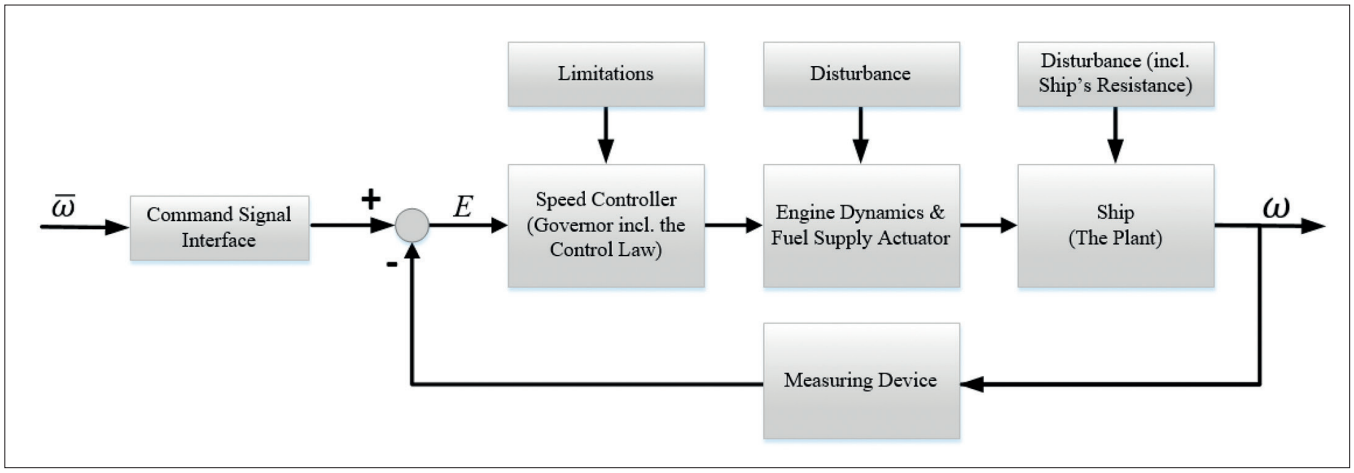

Fig. 3. Block diagram of the control system

$$J_P = \frac{u(1-w)}{\omega_p D_P} \tag{7}$$

Here, t and w are thrust deduction and wake fraction factors, respectively.

ENGINE DYNAMICS

The key set of determinants in this research are the diesel engine dynamics. The dynamics of marine diesel engines has been studied using different models with various levels of detail, such as zero-dimensional, steady-state delayed response, mean value first principle (MVFP), and discrete-events models (DEM) [27, 28]. A complete understanding of the diesel engine performance needs adequate knowledge of the in-cylinders thermodynamic processes. However, once the diesel engine is investigated as a subsystem of a larger system, i.e. in a ship, an in-cylinder model is neither practical nor necessary due to unsatisfactory real-time capability and inappropriate adaptability with the unsteady operating conditions [29]. Quasi-steady delayed engine dynamics are employed in this study, which is governed by the following differential equation [30]:

$$T_E \dot{Q}_E(t-\tau) + Q_E(t-\tau) = K_E X_f(t) \tag{8}$$

where T_E, τ, K_E, and X_f are engine time constant; response delay; gain factor; and fuel flow rate in kg/s, respectively. The time constant reflects the inertial behaviour of the engine for generating torque after receiving the necessary fuel for combustion and is approximated as 90% of the time between two successive ignitions in one cylinder.

$$T_E = 0.9 \cdot \frac{2\pi}{\omega_E} \tag{9}$$

The time delay is determined as half of the time needed for two successive ignitions:

$$\tau = \frac{1}{2} \cdot \frac{2\pi}{Z_E \omega_E} \tag{10}$$

where ω_E and Z_E are angular shaft velocity and the number of engine's cylinders, respectively. The transfer function of the engine dynamics is directly used in the speed control system.

$$\frac{Q_E(S)}{X_f(S)} = \frac{K_E}{1+T_E S} e^{-\tau s} \tag{11}$$

The recommended model requires that the time constant of the engine is higher than the time constant of the exciting force fluctuation, e.g. added resistance. Therefore, the engine can be effectively simulated using this quasi-steady model and can be directly included in a general system of equations as follows:

$$\begin{cases} T_n(t) - R_C(u(t)) - R_A(u(t)) = (\Delta + x_{\dot{u}})\dot{u}(t) \\ Q_E(t) - Q_P(t) = (I_P + I_{Pa} + I_E + I_S)\dot{\omega}(t) \\ T_E \dot{Q}_E(t-\tau) + Q_E(t-\tau) = K_E X_f(t) \end{cases} \tag{12}$$

Regarding the selected full-scale ship and the corresponding propeller, a MAN-B&W 8S65ME-C8.5 low-speed diesel engine is chosen as the prime mover with a Service Maximum Continuous Rating (SMCR) of 19,433 kW at 92.8 RPM. The steady state specification of the selected engine is publicly accessible [24].

Controller implementation

Engines exhibit an immediate response as feedback of any changes in the rate of injected fuel, even for rapid and small changes. Thus, the primary component which controls diesel engines is the fuel rate. The fuel rate in diesels engines is controlled using different techniques, but primarily with speed governors. The selected engine in the present study is also assumed to be equipped with a governor. Different control strategies are available for controlling the diesel engine. Captains usually prefer to maintain a constant shaft speed while sailing. Thus, the controller is designed based on this strategy, with a schematic of the control system block diagram shown Fig. 3.

The controller receives a set-point signal which is defined as the shaft speed corresponding to the steady state operating condition of the engine, $\bar{\omega}$. This set-point forces the engine to continuously operate at its Maximum Continuous Rating (MCR) condition regardless of the sea conditions. The controlled signal, ω, is the instantaneous shaft speed and is designed as the feedback signal. Thus, the error signal, E, is defined as

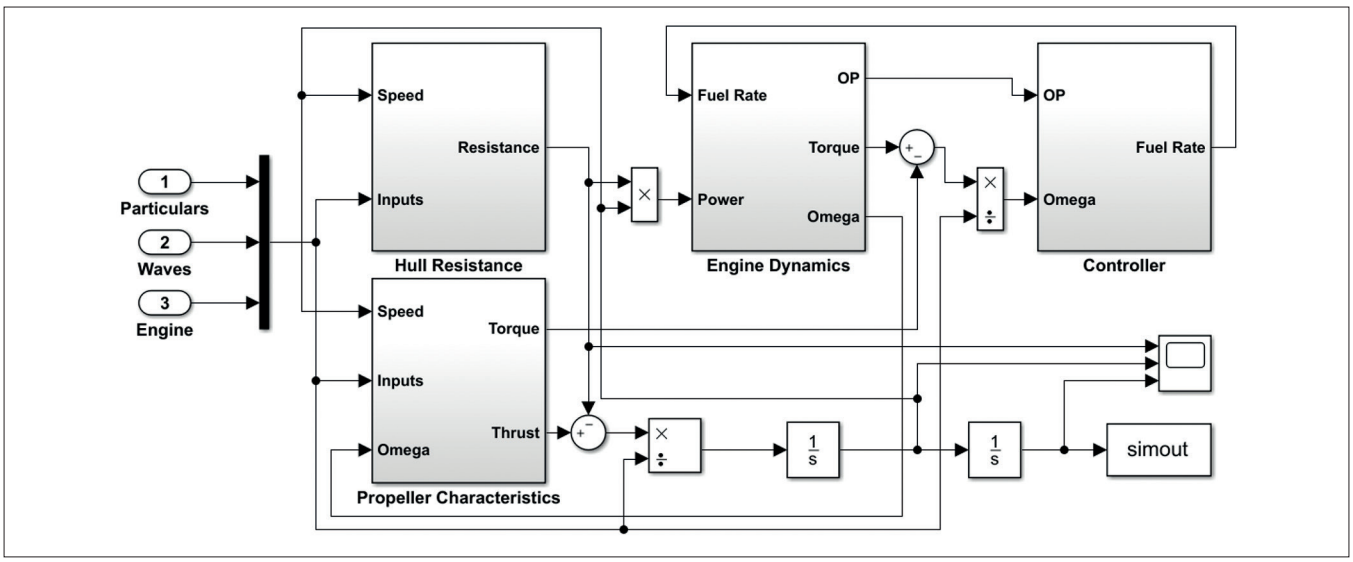

Fig. 4. Block diagram of the whole ship system established in Simulink

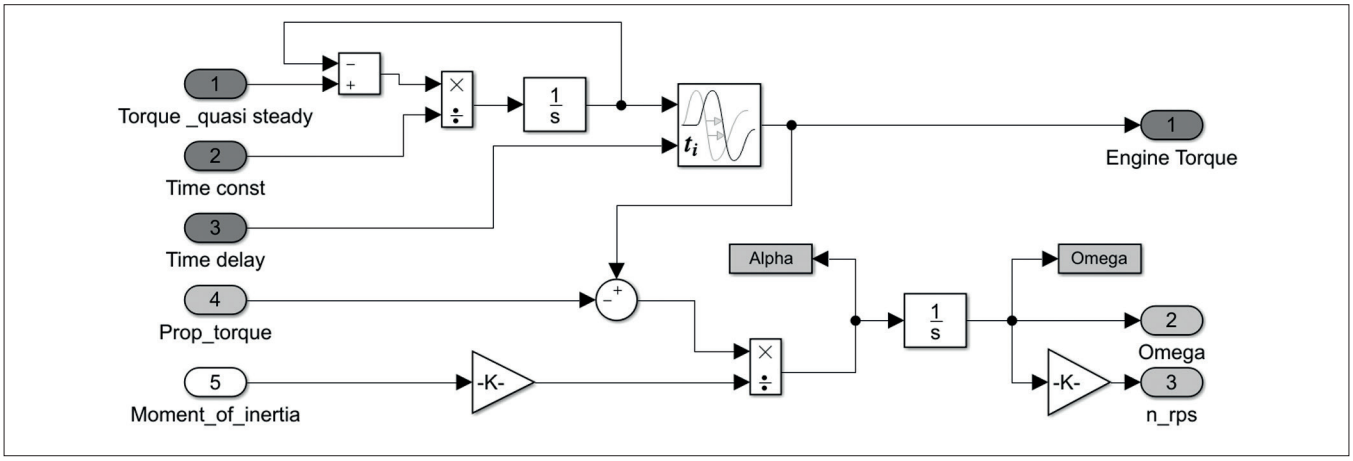

Fig. 5. The internal subsystem of computing unsteady engine dynamics

$$E = \bar{\omega} - \omega \tag{13}$$

The obtained error signal is then amplified and filtered for noise reduction. The processed error signal is fed into the speed governor. The present governor is modelled as a proportional-integral type (PI-action) controller based on the concept of the common diesel engine governors [31]. A proportional-integral-derivative (PID) block with zero derivation gain is employed for the simulation of the governor's performance. The proportional and integrator gains are tuned using a varied Ziegler-Nichols method [32] to account for different sailing scenarios. The output of the governor block is the instantaneous fuel rate of the engine. According to this produced fuel rate signal, the engine performance is adapted for reducing the error signal at each time step. To simulate the ship performance as an integrated system in general, other subsystems apart from the engine and its controller should also be modelled. These subsystems involve the hull resistance, propeller characteristics, and the interconnecting signals. The architecture of the subsystems and the coupling techniques are determined using the governing system of equations and related subsystem formulas as depicted in control block diagram of Fig. 4.

The ship resistance and propeller characteristics are evaluated using given data at the current time step. These characteristics stand as the initial conditions for estimation of the engine dynamics. The results are specified as the input signals of the controller. The controller computes the required fuel rate based on the value of input and error signals. Once the fuel rate is computed by the controller, this rate is fed back to the engine. This loop continues at each time step to reach a converged result. Computation of the engine torque is performed at two other subsystems defined as "*Engine Dynamics*" shown in Fig. 4. At the first step, the steady torque of the engine, e.g. quasi-steady torque, is interpolated from the engine steady-state performance. This quasi-steady torque is then called by another internal subsystem to evaluate its unsteady value based on Eq. (10) as depicted in Fig. 5.

RESULTS AND DISCUSSIONS

To investigate the performance of the governor, two simulations were conducted. The first involved activating the governor so the fuel rate is determined by the controller and

in the second the governor was deactivated with manually forced fuel rates.

GOVERNOR ACTIVATED

The simulations are systematically carried out for separate scenarios, as summarized in Table 4. Fig. 6 indicates the results of the simulations for Scenarios #1 and #3.

Tab. 4. Different scenarios of fuel consumption at the present study

Scenarios	Sea conditions	Engine operating point (OP)	Objective
#1	Calm	100%	Max. speed
#2	Calm	10%~100%	Ship performance
#3	Calm–Waves	100%	Sailing in waves
#4	Calm–Waves–Calm	100%	Controller response
#5	Calm–Waves–Calm	80% in waves	Speed reduction
#6	Calm–Waves–Calm	Varies	Sustain speed
#7	Calm	Varies	Max. acceleration
#8	Waves	Varies	Governor performance

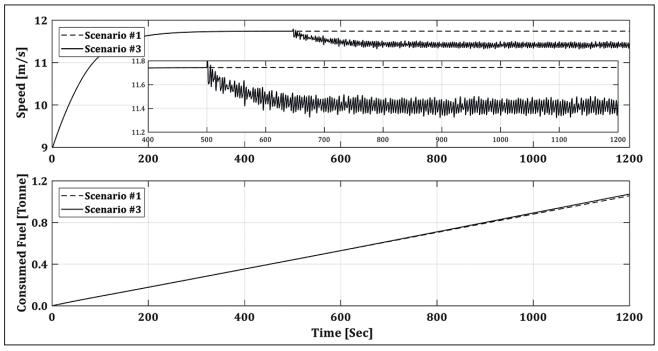

Fig. 6. The overall ship response for scenarios #1 and #3

In the first scenario indicated by the dashed line in Fig. 6, the ship starts with an initial speed of 8.9 m/s and attains a steady state speed of 11.7 m/s. More than 95% of this speed increase occurs in the first 200 seconds. This is clear evidence of the controller performance. The ship consumes about 1.1 tonnes of fuel at the rate of 0.88 kg/s, i.e., 76 MT/day. The ship meets the waves at a speed of 11.74 m/s in the third scenario after 500 seconds of sailing in the calm waters and the speed reduces to 11.4 m/s 300 seconds later. This speed reduction is called involuntary speed reduction. Fuel consumption is essentially identical in both scenarios because of the identical OPs. Fig. 7 shows the results obtained from Scenario #2 when investigating ship performance under different operating conditions.

The ship speed decreases from 11.7 m/s to 6.1 m/s when the operation point reduces from 100% to 10%. Furthermore, the engine power and shaft speed reduce from 19 MW to 1.9 MW and 92.8 RPM to 43.1 RPM, respectively. Fig. 8 illustrates the performance of the engine at different operating conditions.

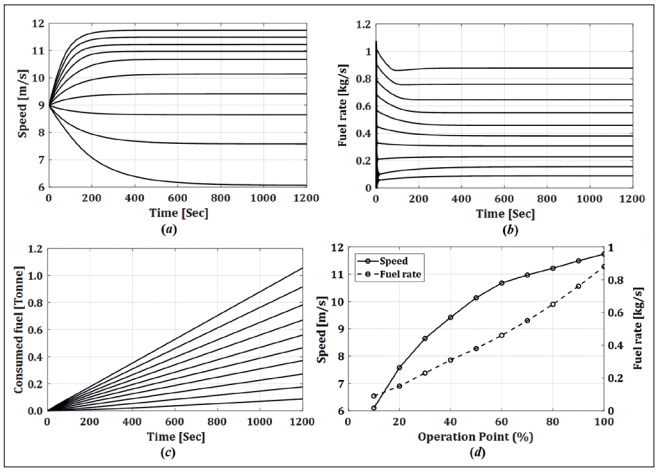

Fig. 7. Overall ship performance for different engine operating points. a) time history of ship speed, b) instantaneous fuel rate, c) overall consumed fuel, and d) variation of ship speed and fuel rate versus different operating points. The operating points reduce from 100% to 10% downward in figures a, b, and c

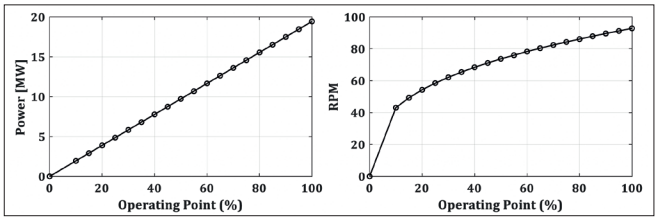

Fig. 8. Engine performance at its different operating points

Fig. 9. shows the response of the controller for different sea conditions in the fourth scenario. The results show that the speed of the ship before and after the waves is the same, indicating the successful trace of different sea conditions by the controller.

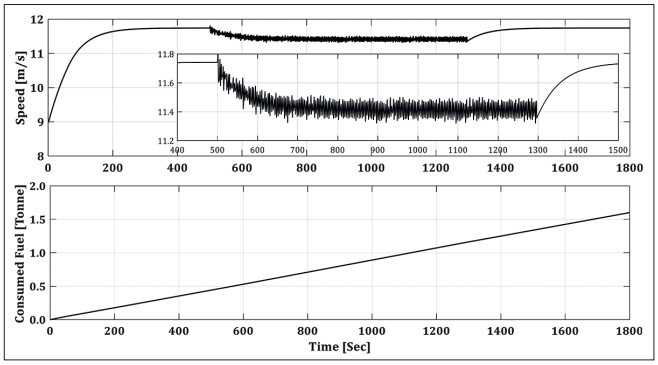

Fig. 9. Controller response for different conditions studied in Scenario #4

The stimulated structural load on the ship hull during sailing in waves is a function of the ship speed. Therefore, captains commonly decide to decrease the ship speed in waves, usually between 0.5 to 4 knots slower than the service speed, in a process known as voluntary speed reduction. This prevents excess loads on the hull. Scenario #5 studies a 20% reduction in engine operating point once the ship encounters waves which cause a 0.5 m/s speed reduction, as shown in Fig. 10. To compare the performance of the controller between Scenarios #3 and #5, the fuel rates are also reported. The patterns of both rates are similar but with different magnitudes.

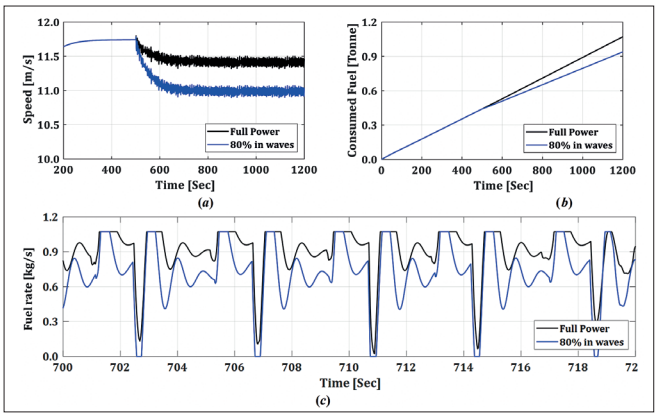

Fig. 10. Simulation results of Scenario #5 defined as voluntary speed reduction in waves compared with the results of Scenario #3. a) Ship speed, b) consumed fuel, and c) fuel rates reported for a typical interval of 20 seconds

In Scenario #6 the ship is initially moving in calm waters and then in waves. The controller's mission is to increase the operating point so that the ship's speed is constant across travelling in waves and in calm waters, as presented in Fig. 11. This shows that the ship speed can be sustained by increasing the engine power by just 4%.

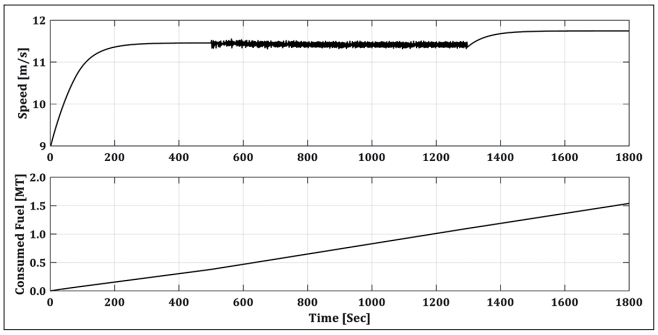

Fig. 11. Sustaining the ship speed in waves introduced in Scenario #6

Fig. 12 shows the simulation results for Scenario #7. Two separate accelerating and decelerating manoeuvres with the same extremums are defined. The results show that the ship speed increased from 6.1 to 11.74 m/s in 300 seconds with an acceleration of about 0.02 m/s^2. However, the ship deceleration takes three times longer with a deceleration of about 0.006 m/s^2. This scenario is a classic study of a controller response to a step function.

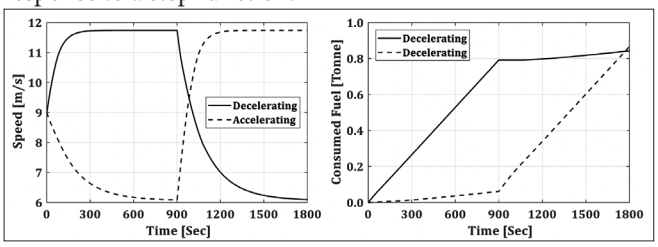

Fig. 12. Evaluation of the ship performance in successive accelerating motions

The voyage distance for different scenarios can be used for the estimation of fuel consumption as a function of travelled distance, which is defined by the parameter Γ and is depicted in Fig. 13. Once the fuel price per unit volume and the voyage distance are known, the crucial fuel cost of shipping can be readily estimated.

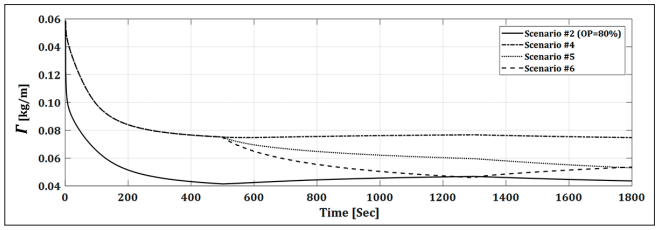

Fig. 13. Instantaneous values of for different shipping scenarios

GOVERNOR DEACTIVATED

The governor is deactivated in the second series of the results. The fuel rates are set to predefined profiles to find any possible reduction in fuel consumption while moving in waves. These rates include constant, sinusoidal, and square rates. Fig. 14 displays the first attempt. Here, the fuel rate is defined as a constant function, with the time averaged rate of 0.902 kg/s used, as obtained from Scenario #4. The solver uses this rate as an initial value and changes it to find the same ship speed in waves. Fig. 15 depicts the results of this simulation via the reported fuel rates. The solver finds the constant value of 0.905 kg/s to attain the same speed, namely 0.4% more than timeaveraged value.

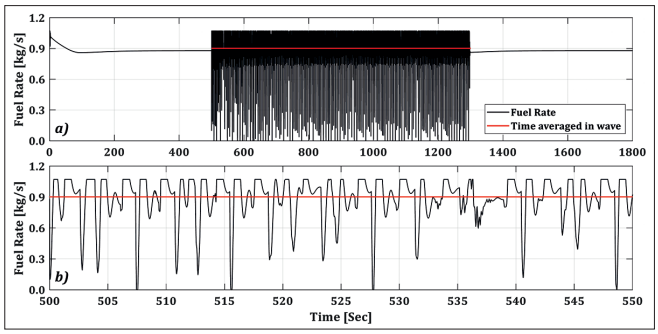

Fig. 14. a) Instantaneous fuel-rate for scenario #4 and its time averaged in waves, b) the magnified view

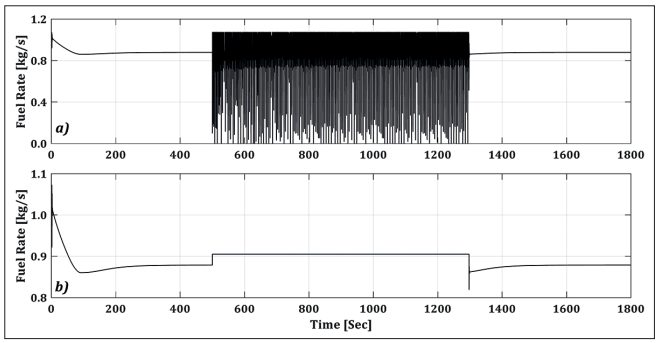

Fig. 15. Comparison of fuel rates, a) controlled by governor, b) forced constant rate

The results show that the governor can be completely turned off during motion in waves. However, it is crucial to note that this does not imply that the controller can be removed from the system. Without a proper controller, the fuel consumption is dramatically increased under different ship operating conditions. A synchronized presentation of the fuel rate and the total resistance is illustrated in Fig. 16. Once the controller finds any local oscillation is the resistance, it immediately changes

the fuel rate to keep the propeller shaft speed constant. The controller responds to the resistance excitation with a very short time delay, as defined by Eq. (12).

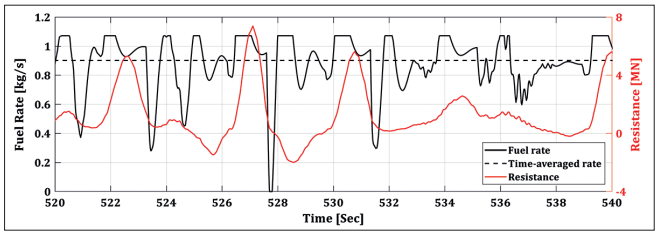

Fig. 16. Synchronized representation of time histories of the fuel rate computed by the controller and the total resistance

Other rates with sinusoidal and square behaviour are also generated with the same peaks and the same time-averaged rate according to those shown in Fig. 14. However, different frequencies are used to find any possible correlation between the fuel consumption and the frequencies, as presented in Fig. 17. The computed fuel consumption is normalized using the steady state fuel consumption that is evaluated at the end of motion in waves in scenario #4, defined as η. It is shown that there is no correlation between these parameters.

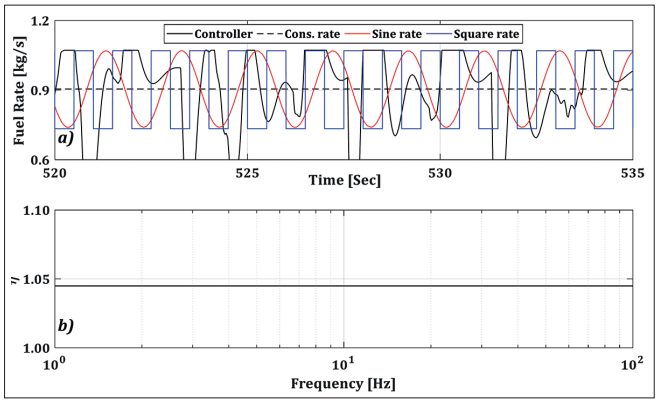

Fig. 17. Different forced fuel rates, a) Typical fuel rate profiles, b) normalized fuel consumption for forced periodic fuel rates with different frequencies

CONCLUSION

The overall ship performance, particularly real-time fuel consumption, is investigated using a new hull-engine-propeller interaction model under different sea conditions. Various voyage scenarios are studied to identify any correlation between fuel consumption and ship dynamics. The results show that the employed controller successfully responds to different challenging scenarios with reasonable performance. Additionally, the benefit of a constant forced fuel rate is illustrated in comparison with the high oscillating response of the governor during motion in waves. Voluntary and involuntary ship speed reductions in waves are introduced, and it is concluded that the proposed model can accurately simulate such speed reductions. Moreover, the capability of the recommended model and simulation framework to predict the instantaneous and total cost of consumed fuel per voyage is also noted. This work offers a practical tool which can be utilized in all stages of ship design and can be implemented to help manage the energy efficiency of existing ships.

REFERENCES

1. United Nations, "UN Handbook of Statistics." Geneva, 2021.
2. Y. Du et al., "Two-phase optimal solutions for ship speed and trim optimization over a voyage using voyage report data," Transportation Research Part B, vol. 122, pp. 88-114, 2019, doi: 10.1016/j.trb.2019.02.004.
3. Coraddu et al., "Vessels fuel consumption forecast and trim optimisation: A data analytics perspective," Ocean Engineering, vol. 130, pp. 351–370, 2017, doi: 10.1016/j.oceaneng.2016.11.058.
4. R. Lu, O. Turan, E. Boulougouris, C. Banks, and A. Incecik, "A semi-empirical ship operational performance prediction model for voyage optimization towards energy efficient shipping," Ocean Engineering, vol. 110, pp. 18-28, 2015, doi: 10.1016/j.oceaneng.2015.07.042.
5. L. Þ. Leifsson, H. Sævarsdóttir, S. Þ. Sigurðsson, and A. Vésteinsson, "Grey-box modeling of an ocean vessel for operational optimization," Simulation Modelling Practice and Theory, vol. 16, no. 8, pp. 923–932, 2008, doi: 10.1016/j.simpat.2008.03.006.
6. P. Karagiannidis and N. Themelis, "Data-driven modelling of ship propulsion and the effect of data pre-processing on the prediction of ship fuel consumption and speed loss," Ocean Engineering, vol. 222, 2021, doi: 10.1016/j.oceaneng.2021.108616..
7. L. Yang et al., "A genetic algorithm-based grey-box model for ship fuel consumption prediction towards sustainable shipping," Annals of Operations Research, pp. 1-27, 2019, doi: 10.1007/s10479-019-03183-5.
8. H. Lee et al., "A decision support system for vessel speed decision in maritime logistics using weather archive big data," Computers & Operations Research, vol. 98, pp. 330–342, 2018, doi: 10.1016/j.cor.2017.06.005.
9. Y. Denev, "Retrofitting the Bow of a General Cargo Vessel and Evaluating Energy Efficiency Operational Index", Polish Maritime Research, vol. 30, no. 4, pp. 17–23, Dec. 2023, doi: 10.2478/pomr-2023-0054.
10. F. Tillig et al., "A generic energy systems model for efficient ship design and operation," Proceedings of the Institution of Mechanical Engineers, Part M: Journal of Engineering for the Maritime Environment, vol. 231, pp. 649–666, 2017, doi: 10.1177/1475090216680672.

11. P. Gusti et al., "Reduction in ship fuel consumption and emission by sailing at slow speeds," Journal of Engineering Science and Technology, vol. 14, no. 6, pp. 3267–3281, 2019.

12. R. Vettor and C. G. Soares, "Development of a ship weather routing system," Ocean Engineering, vol. 123, pp. 1–14, 2016, doi: 10.1016/j.oceaneng.2016.06.035.

13. S. Wang and X. Wang, "A polynomial-time algorithm for sailing speed optimization with containership resource sharing," Transportation Research Part B: Methodological, vol. 93, pp. 394–405, 2016, doi: 10.1016/j.trb.2016.08.003.

14. L. P. Perera, B. Mo, and L. A. Kristjánsson, "Identification of optimal trim configurations to improve energy efficiency in ships," in 10th IFAC Conference on Manoeuvring and Control of Marine Craft, 2015, pp. 267–272.

15. O. Kanifolskyi, "General Strength, Energy Efficiency (EEDI), and Energy Wave Criterion (EWC) of Deadrise Hulls for Transitional Mode", Polish Maritime Research, vol. 29, no. 3, pp. 4–10, Sep. 2022, doi: 10.2478/pomr-2022-0021.

16. U. Larsen et al., "Development of a model for the prediction of the fuel consumption and nitrogen oxides emission trade-off for large ships," Energy, vol. 80, pp. 545-555, 2015, doi: 10.1016/j.energy.2014.12.009.

17. Q. Yin et al., "Design of a real-time ship fuel consumption monitoring system with self-checking function," in 4th International Conference on Transportation Information and Safety, Banff, Canada, 2017, pp. 735–738.

18. E. Sandvik et al., "Estimation of fuel consumption using discrete-event simulation - a validation study," in Marine Design XIII, P. Kujala, Ed., Helsinki: CRC Press, 2018.

19. N. Degiuli et al., "Increase of Ship Fuel Consumption Due to the Added Resistance in Waves," Sustainable Development of Energy, Water and Environment Systems, vol. 5, no. 1, pp. 1–14, 2017, doi: 10.13044/j.sdewes.d5.0129.

20. F. Tilling and J. W. Ringsberg, "A 4 DOF simulation model developed for fuel consumption prediction of ships at sea," Ships and Offshore Structures, 2018.

21. C. G. Rodriguez, M. I. Lamas, J. D. Rodriguez, and A. Abbas, "Analysis of the Pre-Injection System of a Marine Diesel Engine Through Multiple-Criteria Decision-Making and Artificial Neural Networks", Polish Maritime Research, vol. 28, no. 4, pp. 88–96, Jan. 2022, doi: 10.2478/pomr-2021-0051.

22. R. Varbanets et al., "Concept of Vibroacoustic Diagnostics of the Fuel Injection and Electronic Cylinder Lubrication Systems of Marine Diesel Engines", Polish Maritime Research, vol. 29, no. 4, pp. 88–96, Dec. 2022, doi: 10.2478/pomr-2022-0046.

23. Q. Shi, Y. Hu, and G. Yan, "Hierarchical Multiscale Fluctuation Dispersion Entropy for Fuel Injection System Fault Diagnosis", Polish Maritime Research, vol. 30, no. 1, pp. 98–111, Mar. 2023, doi: 10.2478/pomr-2023-0010.

24. M. H. Ghaemi and H. Zeraatgar, "Analysis of hull, propeller and engine interactions in regular waves by a combination of experiment and simulation," Journal of Marine Science and Technology, vol. 26, pp. 257–272, 2021, doi: 10.1007/s00773-020-00734-5.

25. F. P. Arribas, "Some methods to obtain the added resistance of a ship advancing in waves," Journal of Ocean Engineering, vol. 34, pp. 946–955, 2007, doi: 10.1016/j.oceaneng.2006.06.002.

26. O. M. Faltinsen et al., "Prediction of Resistance and Propulsion of a Ship in a Seaway," in Proceedings of the 13th Symposium on Naval Hydrodynamics, Tokyo, Japan, 1980, pp. 505–529.

27. J. B. Heywood, "Internal combustion engine fundamentals." USA: Mc-Graw Hill, 1988.

28. M. H. Ghaemi, "Performance and emission modelling and simulation of marine diesel engines using publicly available engine data," Polish Maritime Research, vol. 28, no. 4, pp. 63-87, 2021, doi: 10.2478/pomr-2021-0050.

29. J. B. Woodward and R. G. Latorre, "Modeling of diesel engine transient behavior in marine propulsion analysis," Society of Naval Architects and Marine Engineers-Transactions, 1984, vol. 92.

30. M. H. Ghaemi, "Changing the ship propulsion system performances induced by variation in reaction degree of turbocharger turbine," Journal of Polish CIMAC, vol. 6, pp. 55–70, 2011.

31. N. Xiros, "Robust Control of Diesel Ship Propulsion." London: Springer, 2002.

32. G. Ellis, "Control System Design Guide." Elsevier, 2012.